Available online at www.sciencedirect.com
SciVerse ScienceDirect
Ceramics International 39 (2013) S461–S464
CERAMICS INTERNATIONAL
www.elsevier.com/locate/ceramint

Structural and electrical properties of sol–gel-derived Al-doped bismuth ferrite thin films

Dahua Zhang, Peng Shi*, Xiaoqing Wu, Wei Ren

Electronic Materials Research Laboratory, Key Laboratory of the Ministry of Education and International Center for Dielectric Research, Xi'an Jiaotong University, Xi'an 710049, China

Available online 16 October 2012

Abstract

Al-doped $BiFeO_3$ ($BiFe_{(1-x)}Al_xO_3$) thin films with small doping content ($x=0$, 0.05, and 0.1) were grown on $Pt(111)/TiO_2/SiO_2/Si$ substrates at the annealing temperature of 550 °C for 5 min in air by the sol–gel method. The crystalline structure, as well as surface and cross section morphology were studied by X-ray diffraction and scanning electron microscope, respectively. The dielectric constant of $BiFeO_3$ film was approximately 71 at 100 kHz, and it increased to 91 and 96 in the 5% and 10% Al-doped $BiFeO_3$ films, respectively. The substitution of Al atoms in $BiFeO_3$ thin films reduced the leakage current obviously. At an applied electric field of 260 kV/cm, the leakage current density of the undoped $BiFeO_3$ films was 3.97×10^{-4} A/cm^2, while in the 10% Al-substitution $BiFeO_3$ thin films it was reduced to 8.4×10^{-7} A/cm^2. The obtained values of $2P_r$ were 63 μC/cm^2 and 54 μC/cm^2 in the 5% and 10% Al-doped $BiFeO_3$ films at 2 kHz, respectively.
© 2012 Elsevier Ltd and Techna Group S.r.l. All rights reserved.

Keywords: $BiFeO_3$; Thin films; Al-doped; Leakage current

1. Introduction

$BiFeO_3$ is a lead-free material with a high Curie temperature ($T_c=850$ °C) and a giant remanent polarization ($P_r=146$ μC/cm^2) [1,2], and it is a promising material for high-density ferroelectric random access memory [3]. The lattice structure of $BiFeO_3$ crystal is rhombohedral perovskite, which belongs to the R3c space group with unit cell parameters $a_r=5.364$ Å and $\alpha_\gamma=0.6°$ [4]. However, the major problems of $BiFeO_3$ films are the low electrical resistivity and large leakage current, which affect the ferroelectric properties at room temperature. The relatively high conductivity of $BiFeO_3$ films is known to be attributed to the variable oxidation states of Fe ions, Fe^{3+} and Fe^{2+}, which cause oxygen vacancies and produce electron hopping in films [5,6]. Many efforts have been made to reduce the leakage current of $BiFeO_3$ films and to improve the ferroelectric properties. One of the effective ways is by doping of ions at A(Bi) site, B(Fe) site or AB site. From the literature, Tb [7], La [8,9], Ce [10], Eu, Gd, Dy [11] doping at Bi-site and Ti [5], Cr [12], Zr [13], Mn [14] at Fe-site in $BiFeO_3$ thin films, could stabilize the valency of Fe^{3+}, greatly reducing its leakage current and highly enhancing ferroelectric properties. $BiAlO_3$ is a new excellent ferroelectric material with R3c symmetry. It shows a large spontaneous polarization of 76 μC/cm^2, and the Curie temperature is about 530 °C [15,16]. Therefore, it is necessary to investigate the preparation and electric properties of Al-doped $BiFeO_3$ thin films. In this paper, the electric properties and leakage current density were investigated by introducing Al ion into the $BiFeO_3$ thin films. The hysteresis loop and PUND curves were measured to study the ferroelectric properties of the Al-doped $BiFeO_3$ films with small doping content.

2. Experimental procedures

For the preparation of Al-doped $BiFeO_3$ ($BiFe_{(1-x)}Al_xO_3$) precursor solution, iron nitrate nonahydrate $[Fe(NO_3)_3\cdot 9H_2O]$, bismuth nitrate · pentahydrate $[Bi(NO_3)_3\cdot 5H_2O]$ and aluminum nitrate nonahydrate $[Al(NO_3)_3\cdot 9H_2O]$ were used as starting chemicals. 2-Methoxyethanol was selected as the

*Corresponding author. Tel.: +86 39 82668679; fax: +86 29 82668794.
E-mail address: spxjy@mail.xjtu.edu.cn (P. Shi).

0272-8842/$ - see front matter © 2012 Elsevier Ltd and Techna Group S.r.l. All rights reserved.
http://dx.doi.org/10.1016/j.ceramint.2012.10.114

solvent. The bismuth nitrate, iron nitrate and aluminum nitrate were dissolved in 2-methoxyethanol by stirring for 30 min at room temperature. Then the above three solutions were mixed in mole ratio of Bi:($Fe_{(1-x)}Al_x$)=1:1, with x=0%, 5% and 10%. The final mixtures were stirred for 3 h at room temperature to make homogeneous solutions. The concentration of the solutions was adjusted to 0.3 mol/L by adding 2-methoxyethanol. The films were deposited by spin coating at 3000 rpm for 30 s. The as-deposited wet films were dried at 350 °C for 4 min, and then annealed at 550 °C for 5 min in air by a rapid thermal annealing method. The process of spin coating and annealing was repeated for several times to obtain the desired thickness. For electric measurements, Pt top electrodes of 0.5 mm diameter were deposited on the surface of the films by a sputtering method through a shadow mask. Then the films with Pt electrodes were heated at 300 °C for 10 min in an oven to improve adhesion between metal and film.

Microstructure and crystallization of films were investigated by a JEOL JSM-7000F field emission scanning electron microscope (FESEM) and a Rigaku D/MAX-2400 X-ray diffractometer (XRD). The dielectric properties were measured with an Agilent 4294A LCR meter. *J–E* leakage current density characteristics were measured with a Keithley 4200. Polarization–electric field (*P–E*) hysteresis loops were characterized with a TF Analyzer2000 standardized ferroelectric test system (AixACCT Systems).

3. Results and discussions

Fig. 1 shows the XRD patterns of $BiFe_{(1-x)}Al_xO_3$ (x=0, 0.05, 0.1) films on $Pt/Ti/SiO_2/Si(100)$ substrates annealed at 550 °C for 5 min by rapid thermal processing. As observed in Fig. 1, all films showed perovskite structure and were polycrystalline with no evidence of preferential orientation. From the XRD results, the lattice constant of $BiFe_{(1-x)}Al_xO_3$ films was calculated by Scherrer's equation

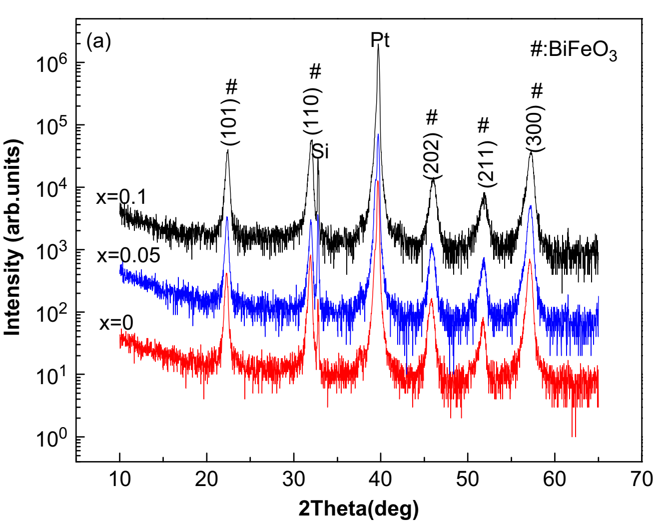

Fig. 1. XRD pattern of $BiFe_{(1-x)}Al_xO_3$ (x=0, 0.05, 0.1) thin films annealed at 550 °C by RTA processing.

as 3.956 Å, 3.953 Å, 3.942 Å, for x=0, 0.05, and 0.1, respectively. The lattice constant became smaller with the increase of Al doping, because the radius of Al^{3+}(0.57 Å) is smaller than that of Fe^{3+}(0.67 Å).

The surface morphology of the $BiFe_{(1-x)}Al_xO_3$ thin films was studied by FESEM. Fig. 2 shows the SEM photos of $BiFe_{(1-x)}Al_xO_3$ films. From the SEM photos, it can be seen that the films were about 650 nm in thickness, and the interface between the films and Pt sub-electrode was clear. The surface SEM pictures indicated that all films were well grown polycrystalline films. The pure $BiFeO_3$ film showed larger grain size and having more porosity than those of the Al-doped films. With the Al doping, the films became denser. Therefore, Al substitution had substantially reduced the average grain size, which improved the surface morphology, and this phenomenon had corresponded to the AFM results (not shown here). From the AFM results, the root mean square (RMS) roughnesses were calculated to be 4.62 nm, 3.63 nm and 3.61 nm for the surface of the $BiFe_{(1-x)}$ Al_xO_3 films (x=0, 0.05, 0.1), respectively.

The frequency dependences of dielectric constant (ε_γ) and dielectric loss (tan δ) of the $BiFe_{(1-x)}Al_xO_3$ films at the frequencies of 100 Hz–1 MHz at room temperature are shown in Fig. 3. The relatively lower dielectric constant measured in this work could be due to the small grain size of the film. The dielectric constants increased with the increase of Al content. The measured dielectric constant and dielectric loss of $BiFe_{(1-x)}Al_xO_3$ (x=0, 0.05, 0.1) thin films at 100 kHz were 77, 91, 96 and 1.03%, 1.15%, 1.11%, respectively. The films with higher dielectric losses at lower frequencies contributed to the effect of the space charge at the interface [17].

Fig. 4 shows the *J–E* leakage current density versus applied field characteristic of the $BiFe_{(1-x)}Al_xO_3$ films. It can be seen obviously for the whole range of electric field that the leakage current density can be reduced by introducing Al ions into the films. The leakage current density of pure $BiFeO_3$ film was 3.97×10^{-4} A/cm^2 under a positive electric field of 260 kV/cm, while the leakage current densities of $BiFe_{(1-x)}Al_xO_3$ with x=0.1 and x=0.05 were 8.4×10^{-7} A/cm^2 and 5.6×10^{-5} A/cm^2 at the same electric field, respectively. The main reason for the reduction of leakage current density in the films is probably due to the reduction of the oxygen vacancies in the films by the Al-dopants [5,17] and/or the smaller grain size, which is seen from the SEM photos in Fig. 2.

The hysteresis loops for the $BiFe_{(1-x)}Al_xO_3$ films were recorded using polarization hysteresis and pulsed polarization (positive-up-negative-down, PUND) at the frequency of 2000 Hz by using TF Analyzer2000 standardized ferroelectric test system. The measurement results were plotted in Fig. 5. From Fig. 5a, the hysteresis loop of pure $BiFeO_3$ thin film was round due to the large leakage current. However, the Al-doped $BiFeO_3$ thin films showed good ferroelectric hysteresis loop under the same condition relatively. For $BiFe_{(1-x)}Al_xO_3$ (x=0.05, 0.1), the $2P_r$ values

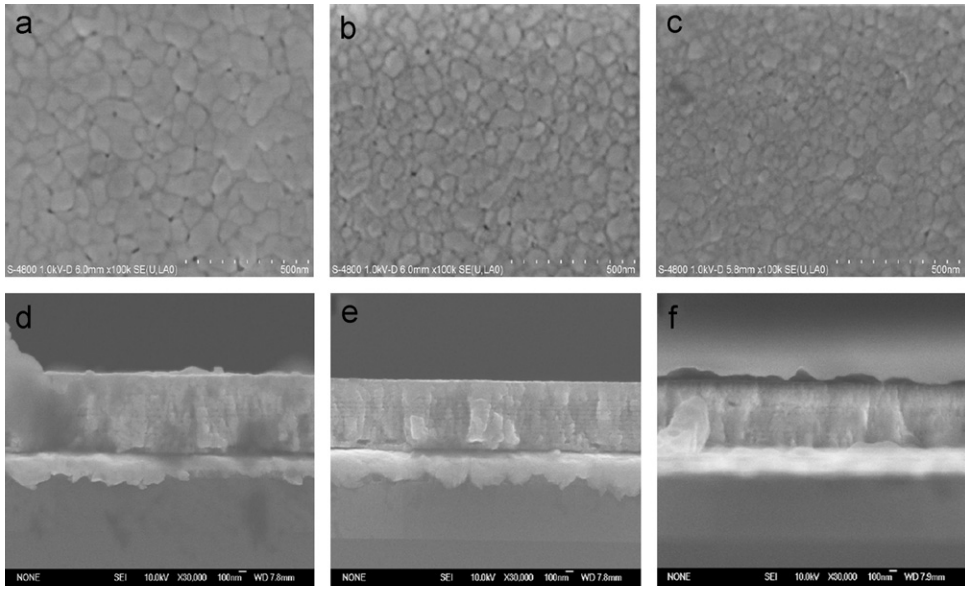

Fig. 2. FESEM photos of the $BiFe_{(1-x)}Al_xO_3$ films: a, b, and c are the surface photos; d, e, and f are the cross section of $BiFe_{(1-x)}Al_xO_3$ ($x=0$, 0.05, 0.1) films.

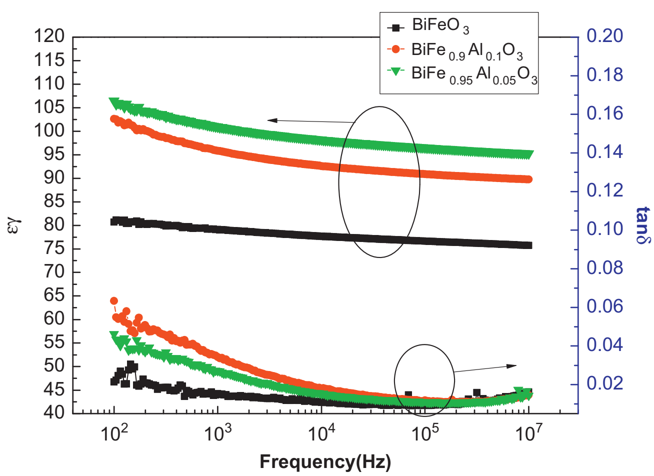

Fig. 3. Frequency dependences of dielectric constant and dielectric loss of the $BiFe_{(1-x)}Al_xO_3$ ($x=0$, 0.05, 0.1) films.

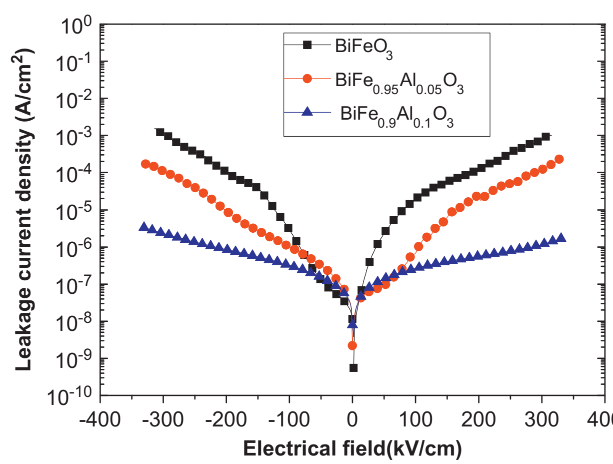

Fig. 4. J–E leakage current density versus applied field of $BiFe_{(1-x)}Al_xO_3$ ($x=0$, 0.05, 0.1) films.

were measured as 63 $\mu C/cm^2$ and 54 $\mu C/cm^2$, while the $2E_c$ were measured as 950 kV/cm and 750 kV/cm, respectively. The large E_c maybe related to domain spinning by space charge [18]. From the literature, the pulsed polarization PUND measurement was less affected by leakage and non-linear dielectric effects [19]. In Fig. 5b, $\Delta P=P_{sw}-P_{nsw}=2P_r$ (P_{sw} is the switched polarization and P_{nsw} is the nonswitched polarization), all films were measured at frequency of 2000 Hz and the write plus time was 20 μs. The measured ΔP of the $BiFeO_3$, $BiFe_{0.95}Al_{0.05}O_3$, and $BiFe_{0.9}Al_{0.1}O_3$ films were 63 $\mu C/cm^2$, 45 $\mu C/cm^2$, 39 $\mu C/cm^2$, respectively. The measured PUND values (ΔP) were smaller than the hysteresis loop values ($2P_r$) for all films, which confirmed that the leakage current contributes to raised $2P_r$. From both the hysteresis loop and PUND curves, the values of $2P_r$ and ΔP were decreased with the increase of Al doping content.

4. Conclusion

$BiFe_{(1-x)}Al_xO_3$ ($x=0$, 0.05, 0.1) thin films were deposited on $Pt(111)/TiO_2/SiO_2/Si$ substrates by the sol–gel method. The introduction of Al ions in the films can reduce the grain size and improve the surface quality of the films. The dielectric constant and dielectric loss of $BiFe_{(1-x)}Al_xO_3$ ($x=0$, 0.05, 0.1) thin films at 100 kHz were 77, 91, 96 and 1.03%, 1.15%, 1.11%, respectively. The leakage current density of the films was reduced obviously with Al doping. While, the Al content was 10% in the films, the leakage current density reached the minimum of 8.4×10^{-7} A/cm^2, which is lesser than that of the pure $BiFeO_3$ film. The measured PUND values of $BiFe_{(1-x)}Al_xO_3$ thin films were 63 $\mu C/cm^2$, 45 $\mu C/cm^2$, 39 $\mu C/cm^2$, for $x=0$, 0.05 and 0.1, respectively.

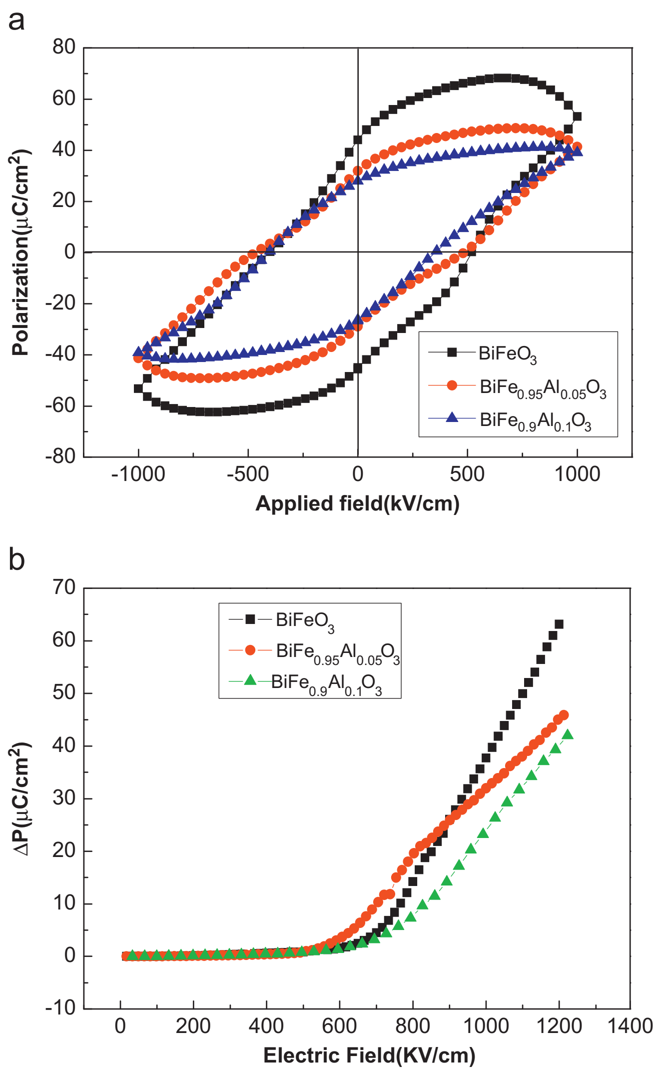

Fig. 5. Ferroelectric behavior of the $BiFe_{(1-x)}$ Al_xO_3 (x=0, 0.05, 0.1) films at 2000 Hz: (a) hysteresis loop and (b) PUND curve.

Acknowledgments

This work is supported by the International Science and Technology Cooperation Program of China (Grant no. 2011DFA51880) and the Shaanxi Province International Collaboration Program (Grant no. 2012KW-02).

References

[1] Gustau Catalan, James F. Scott, Physics and applications of bismuth ferrite, Advanced Materials 21 (24) (2009) 2463–2485.

[2] K.Y. Yun, R. Dan, K. Takeshi, N. Minoru, O. Masanori, Giant ferroelectric polarization beyond 150 μC/cm^2 in $BiFeO_3$ thin film, Japanese Journal of Applied Physics 43 (2004) L647–L648.

[3] J. Wang, J.B. Neaton, H. Zheng, V. Nagarajan, S.B. Ogale, B. Liu, D. Viehland, V. Vaithyanathan, D.G. Schlom, U.V. Waghmare, N.A. Spaldin, K.M. Rabe, M. Wuttig, R. Ramesh, Epitaxial $BiFeO_3$ multiferroic thin film heterostructures, Science 299 (2003) 1719.

[4] F. Kubel, H. Schmid, Structure of a ferroelectric and ferroelastic monodomain crystal of the perovskite $BiFeO_3$, Acta Crystallographica B 46 (1990) 698–702.

[5] X.D. Qi, J. Dho, R. Tomov, Greatly reduced leakage current and conduction mechanism in alivolent-ion-doped $BiFeO_3$, Journal of Applied Physics 86 (2005) 062903.

[6] Z. Cheng, B. Chen, X.J. Xiao, Z.H. Zuo, Y.W. Zuo, Y.F. Fu, Q.F. Zhan, R.W. Li, Local leakage current behaviors of $BiFeO_3$, Chinese Physics B 20 (11) (2011) 117701.

[7] Y. Wang, C.W. Nan, Effect of Tb doping on electric and magnetic behavior of $BiFeO_3$ thin films, Journal of Applied Physics 103 (2008) 024103.

[8] F. Yan, T.J. Zhu, M.O. Lai, L. LU, Enhanced multiferroic properties and domain structure of La-doped $BiFeO_3$ thin films, Scripta Materialia 63 (2010) 780–783.

[9] Z.L. Hu, Y. Wang, J.Y. Dai, D. Zhou, Y.M. Hu, H.S. Gu, K.Z. Baba-Kishi, Enhanced multiferroic properties of La-doped $BiFeO_3$ nanotubes fabricated through anodic alumina template method, Journal of Advanced Dielectrics 1 (2011) 325–330.

[10] Y.Y. Wang, A large polarization in Ce-modified bismuth ferrite thin films, Journal of Applied Physics 109 (2011) 124105.

[11] A. Lahmar, S. Habouti, M. Dietze, C.H. Solterbeck, M. Es-Souni, Effects of rare earth manganities on structural, ferroelectric, and magnetic properties of $BiFeO_3$ thin films, Journal of Applied Physics 94 (2009) 012903.

[12] Y.H. Zhang, S.W. Yu, J.R. Cheng, The study of $BiCr_xFe_{(1-x)}O_3$ thin films synthesized by sol–gel technique, Journal of the European Ceramic Society 30 (2010) 271–275.

[13] J. Wei, D.S. Xue, Effect of non-magnetic doping on leakage and magnetic properties of $BiFeO_3$ thin fithi, Applied Surface Science 258 (2011) 1373–1376.

[14] S.G. Cui, Enhanced ferroelectric properties in $BiFe_{0.95}Mn_{0.05}O_3$ thin films, Journal of Alloys and Compounds 508 (2010) 520–522.

[15] J. Zylberberg, A.A. Belik, T. Muromachi, Z.G. Ye, Bismuth aluminate: a new high-TC lead-free piezo-ferroelectric, Chemistry of Materials 19 (26) (2007) 6385–6390.

[16] J.Y. Son, C.S. Park, Y.H. Shin, Epitaxial $BiAlO_3$ thin film as a lead-free ferroelectric material, Journal of Applied Physics 92 (2008) 222911.

[17] X.Z. Wang, H.R. Liu, B. Yan, Enhanced ferroelectric properties of Ce-substituted $BiFeO_3$ thin films on $LaNiO_3$/Si substrates prepared by sol–gel process, Journal of the European Ceramic Society 29 (2009) 1183–1187.

[18] S.R. Das, R.N.P. Choudhary, P. Bhattacharya, R.S. Katiyar, P. Dutta, A. Manivannan, M.S. Seehra, Structural and multiferroic properties of La-modified $BiFeO_3$ ceramics, Journal of Applied Physics 99 (2006) 066107.

[19] H. Naganuma, Y. Inoue, S. Okamura, Evaluation of electrical properties of leaky $BiFeO_3$ films in high electric field region by high-speed positive-up-negative-down measurement, Applied Physics Express 1 (2008) 061601.